The case against half-metallicity in $La_{0.7}Sr_{0.3}MnO_3$

2007 J. Phys.: Condens. Matter 19 315209

(http://iopscience.iop.org/0953-8984/19/31/315209)

IOP PUBLISHING JOURNAL OF PHYSICS: CONDENSED MATTER

J. Phys.: Condens. Matter **19** (2007) 315209 (15pp) doi:10.1088/0953-8984/19/31/315209

The case against half-metallicity in $La_{0.7}Sr_{0.3}MnO_3$

B Nadgorny

Department of Physics and Astronomy, Wayne State University, Detroit, MI 48201, USA

Received 16 March 2007, in final form 1 April 2007
Published 3 July 2007
Online at stacks.iop.org/JPhysCM/19/315209

Abstract

Half-metallic ferromagnets are universally believed to be of great importance for a multitude of spintronic applications, including non-volatile logic and memory, spin transistors and many other recently proposed devices. While many materials have been predicted to be half-metallic, experimental confirmation of this exciting effect is still very controversial, particularly for optimally doped $La_{0.7}Sr_{0.3}MnO_3$ (LSMO). In this paper we will review some of the techniques used for spin polarization measurements and, in particular, the results obtained for LSMO. It was argued in Nadgorny *et al* (2001 *Phys. Rev.* B **63** 184433) that LSMO is a *transport half-metal*, rather than a conventional half-metal with no minority electrons at the Fermi level at $T = 0$ K. We will discuss some of the more recent measurements in LSMO and see how well this conclusion stacks up against these new results.

(Some figures in this article are in colour only in the electronic version)

1. Half-metals: an introduction

Half-metals were officially introduced in a 1983 paper by de Groot and co-authors [2]. Interestingly, this discovery coincided with the advent of computers which ushered in a new way of doing science, particularly materials science, in which various problems could be solved using a numerical approach. The authors of [2] used the local density approximation (LDA) and found that in some of the so-called Heusler alloys, such as NiMnSb, only one of the energy bands (majority) crosses the Fermi level, E_F, whereas another (minority) has a semiconducting gap in the density of states (DOS). Consequently, this material should be metallic in one spin channel and insulating in another (hence *half*-metal), which means that the electric current will be conducted only by one type of electron (spin-up) and thus would be fully (100%) spin polarized. This unexpected result emphasized the increasing importance of the rapidly developing band structure theory, but simultaneously highlighted some of its limitations. For instance, the vast majority of band structure calculations are based on a single-electron picture [3] and have been performed for the ground state (at $T = 0$ K), while all of the experiments aimed at confirming these predictions are performed at finite temperatures. This raises an important theoretical and practical question: does half-metallicity persist at

finite temperatures? [4]. Most generally the answer to this question is no [4]; moreover, as was recently emphasized in [5], for most metals and metallic oxide half-metals their high spin polarization range is limited to temperatures significantly below the Curie temperature rather than the band gap, which is much more restrictive. Another question which can, at least in principle, be solved within the band structure theory, is the stability of a half-metallic band structure with respect to substitutions and disorder[1] as well as their behaviour at or near the surface, where the translational symmetry is broken. Does the half-metallicity persist all the way up to the surface, or does the surface differ in terms of its band structure properties? While it is well known that one of the main surface effects on the electronic structure is the overall band narrowing due to a smaller coordination number, Z, at the surface, other effects such as surface reconstruction may compete with the band narrowing effect. Conversely, is it possible for a material to be a half-metal only at the surface but not in bulk? A similar question can be asked about the properties of an interface with another materials system which, in addition to having a more complex band structure may also be affected by a high concentration of defects. Many of these important questions do not have unique answers, i.e. they are materials-system dependent.

2. The use of half-metals in spintronics

This unique property of half-metals that simultaneously exhibit metallic and insulating properties at a microscopic level [7] can be utilized in many devices, from memories to new types of logic. It is commonly accepted that finding half-metallic or other highly spin-polarized materials would bring about major advances in spintronics [8], since the performance of practically any device, for example tunnelling magnetoresistance (TMR) devices, improves dramatically as the spin polarization approaches 100% [9], at which point the efficiency of a typical spintronic device $\Delta R/R \rightarrow \infty$; see figure 1. Of course, this conclusion does not reflect completely accurately the real situation, in which spin-flips, spin–orbit interaction, non-zero temperatures, and other spin decoherence effects are bound to reduce the efficiency of any device made of half-metals to make it finite. One might argue, though, that in metals these are relatively small effects and that the efficiency of a device fabricated from a half-metal should still be very high. At the same time, recent advances in interface engineering, such as the use of MgO tunnel barriers [10], has allowed one to use spin filtering in magnetic tunnel junctions to obtain several hundred per cent of the TMR, which, to some extent, has alleviated the need for intrinsically very highly spin polarized materials. We will see, however, that many of these issues cannot be adequately described (and discussed) unless one first accurately defines the concept of spin polarization.

3. What is spin polarization?

Spin polarization P is one of the most important properties of a magnetic system, on a par with the Curie temperature and magnetization. But, while everybody agrees that high spin polarization is crucial for achieving record device efficiencies, the definition of spin polarization is not at all natural, and it is important to recognize this fact before any comparison with different experiments can be made. Strictly speaking, no continuity equation can be written for a spin current (as opposed to a charge current) and thus it can only be defined as an approximation in the limit of small spin–orbit scattering and other spin

[1] For instance, in NiMnSb just 5% of substitutional defects are supposed to be sufficient to reduce its spin polarization dramatically and close the minority gap; see, for instance, [6].

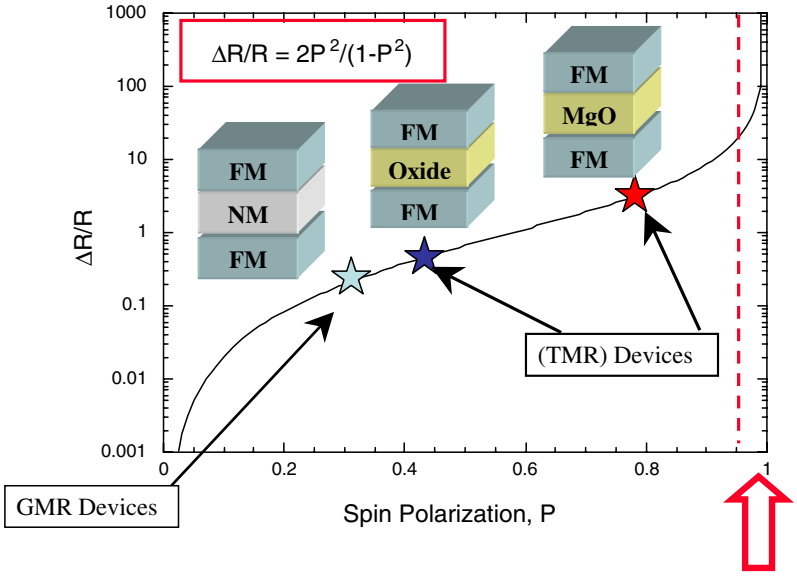

Figure 1. Magnetoresistance $= \frac{\Delta R}{R} = \frac{R_{ap}-R_p}{R_p} = \frac{2P^2}{1-P^2}$ of a tunnelling magnetoresistance (TMR) junction made of the same magnetic materials (R_{ap} and R_p are the resistances corresponding to the parallel and anti-parallel magnetic configurations) as a function of spin polarization, P, determined from the Julliere formula (see [9]). The arrow indicates the desired range of spin polarization values.

decoherence mechanisms. Thus the correct description of spin propagation must involve various spin relaxation processes and/or spin precession [11] and a continuity equation for the charge transfer. One should also recognize a significant difference between metals and semiconductors [12]. In semiconductors the most relevant measure of bulk spin polarization is related to their magnetization, $\boldsymbol{m}$, and the spin polarization P_m can be defined as $P_m = \frac{n_\uparrow - n_\downarrow}{n_\uparrow + n_\downarrow}$ [12], where $n_\uparrow(n_\downarrow)$ is the number of majority (minority) carriers integrated over the filled states. This definition is particularly relevant, as spin–orbit interaction in semiconductors is typically fairly large and in most cases cannot be neglected. On the other hand, in metals and metallic oxides most of the electronic and transport and optical properties are governed by the electronic states at the Fermi level. Therefore, it is predominantly these states, rather than all of the electronic states (that would contribute to the magnetization or magnetic moment density), that must be taken into account. Subsequently, depending on whether we are discussing spectroscopic experiments (such as spin-resolved photoemission) or ballistic or diffusive transport experiments, one can define spin polarizations P_0, P_1, and P_2. P_0 is the spin polarization of the density of states:

$$P_0 = \frac{N_\uparrow(E_F) - N_\downarrow(E_F)}{N_\uparrow(E_F) + N_\downarrow(E_F)},$$

which is most relevant in the spin-resolved photoemission experiments,

$$P_1 = \frac{N_\uparrow(E_F)v_{F\uparrow} - N_\downarrow(E_F)v_{F\downarrow}}{N_\uparrow(E_F)v_{F\uparrow} + N_\downarrow(E_F)v_{F\downarrow}}$$

is the so-called *current carrying* spin polarization [13], which is appropriate in the case of ballistic transport, as in point-contact experiments and spin polarization for the diffusive case,

in which

$$P_2 = \frac{N_\uparrow(E_F)v_{F\uparrow}^2 - N_\downarrow(E_F)v_{F\downarrow}^2}{N_\uparrow(E_F)v_{F\uparrow}^2 + N_\downarrow(E_F)v_{F\downarrow}^2}$$

as in the case of the Bloch–Boltzmann transport equation in the bulk of a ferromagnet [13], where $N_\uparrow(E_F)$, $N_\downarrow(E_F)$ and $v_{F\uparrow}$, $v_{F\downarrow}$ are the majority and minority densities of state (DOS) and Fermi velocities, respectively. P_1 and P_2 are the spin polarizations of the current, which can be introduced in the approximation of negligible spin–orbit interaction. From these definitions it is clear that there need not be any correlation between magnetization and P_0, P_1 and P_2, as magnetization is determined by the sum of all spin states, while the transport spin polarizations, P_1 and P_2, are determined by the DOS convoluted with the Fermi velocity. Specifically, we do not *necessarily* expect to see a monotonic dependence of spin polarization versus magnetization; in fact, they may even have a different sign, as in the case of some 3d-ferromagnets, such as Fe and Ni. This has recently been shown experimentally by using both Meservey–Tedrow spin tunnelling spectroscopy [14, 15] and point-contact Andreev reflection spectroscopy (PCAR) [16]. One can also see that P_0, P_1, P_2, and P_T can be dramatically different (e.g. LSMO band structure calculations predicted $P_0 = 36\%$, whereas $P_2 = 92\%$). Only for a true half-metal (in which $N_\downarrow(E_F) = 0$) do we have $P_0 = P_1 = P_2 = P_T = 100\%$.

4. Comparison of the spin polarization measurement techniques

There are three commonly used techniques for the spin polarization measurements in metals and magnetic oxides: spin-resolved photoemission spectroscopy, the spin-polarized tunnelling (Meservey–Tedrow) technique, and, more recently, the point-contact Andreev reflection (PCAR) technique. Each of these techniques has its own advantages and disadvantages. Photoemission spectroscopy is the most surface-sensitive, probing within 5–20 Å from the surface, which can be very useful for surface studies but may become a drawback if one is mostly interested in the bulk. The energy resolution of the photoemission is generally not as good as the other two techniques, where it is on the order of submillielectronvolts. The Meservey–Tedrow technique has a high energy resolution, but the material under investigation has to be incorporated into a layered structure with a pinhole-free insulating layer between it and a superconducting film. This is a serious limitation of this technique, as some of the most interesting new materials cannot be fabricated in this restrictive geometry. PCAR is perhaps the most flexible in terms of materials that it can study; however, one has to worry about the contact geometry, which is generally not very well defined, as well as possible pressure applied to the sample from a tip that may, in principle, affect the band structure of the material under investigation. The planar Andreev reflection (AR) does not have these problems, but then the interface has to be of high quality in order for Andreev reflection to dominate the interface scattering [17, 18] and the interface resistance has to be higher then the individual in-plane resistance, which is a problem similar to the one encountered in the current-perpendicular-to-plane (CPP) GMR geometry. As we have already mentioned, in spin-resolved photoemission experiments P_0 is measured[2]. PCAR measures P_1 in the ballistic (Sharvin) [19] limit (with the mean free path, L, larger than the contact size, a) and P_2 in the diffusive, or Maxwell, regime ($L < d$), as in the classical Bloch–Bolzmann theory of transport in metals. Tunnelling experiments probe yet another polarization, P_T, which, in the case of a specular barrier of low transparency, is reduced to P_2 as well [20].

[2] In the constant matrix element approximation.

5. Meservey–Tedrow technique

Before addressing a particular materials system (LSMO), we need to make sure that, when we are talking about spin polarization and the spin polarization measurements in different experiments, we mean the same physical quantity [13]. First, one might ask what is the spin polarization introduced in [9] which is plotted in figure 1? Contrary to some of the recent claims in the literature (e.g. [21]), it is not the spin polarization of the density of states, P_0. It becomes clear if one closely follows Julliere's arguments. His derivation was based on Tedrow and Meservey's tunnelling experiments, in which a superconductor/oxide/ferromagnet (S/I/F) junction was used for the spin polarization measurements. The quantity measured in these experiments is the derivative of the tunnelling current as a function of applied voltage. The current can be found using Fermi's golden rule: the electron flux is the product of the density of filled states at a given energy in one of the electrodes and the density of empty states at the same energy in the other electrode, multiplied by the square of the matrix element describing the probability of tunnelling. Thus the current flowing in the positive direction is

$$I\ (V)_+ \approx |M_\uparrow(E)|^2 \int_{-\infty}^{\infty} N_1\ (E - eV) N_2\ (E) f\ (E - eV)[1 - f(E)]\,\mathrm{d}E \quad (1)$$

where $|M_{\uparrow\downarrow}(E)|$ is the tunnelling matrix element with the two subscripts $\uparrow$ and $\downarrow$ corresponding to the majority (minority) electrons, N_1 and N_2 are the respective densities of states, and $f(E)$ is the Fermi function. As the characteristic energy related to superconductivity is of the order of a few millivolts (a typical superconducting gap in a conventional superconductor) and the height of the oxide barriers is on the order of a few volts, the barrier transparency (or $|M_{\uparrow\downarrow}(E)|$) is practically independent of the voltage and therefore its energy dependence can be safely ignored. Similarly, the current in the opposite direction in the same approximation is

$$I(V)_- \approx |M_\downarrow(E)|^2 \int_{-\infty}^{\infty} N_1\ (E - eV) N_2(E) f(E)[1 - f(E - eV)]\,\mathrm{d}E. \quad (2)$$

There is no reason, however, to assume that the two tunnelling matrix elements ($|M_\downarrow(E)|$ and $|M_\uparrow(E)|$) are the same, as generally minority and majority carriers do not come from the same electronic bands and thus can have very different masses and tunnelling probabilities (e.g. the majority may be heavier d-electrons, while the minority may be lighter s-electrons). If we neglect spin–orbit scattering and spin accumulation in a superconductor, the following expression for the conductance in a magnetic field H can be written (by subtracting (1) and (2) and taking the derivative with respect to voltage):

$$G = \frac{\mathrm{d}I}{\mathrm{d}V} \sim N_\uparrow \left|M_\uparrow(E)\right|^2 \int_{-\infty}^{\infty} N_{s\uparrow}(E, H) f'(E + eV)\,\mathrm{d}E - N_\downarrow \left|M_\downarrow(E)\right|^2 \int_{-\infty}^{\infty} N_{s\downarrow}(E, H) f'(E + eV)\,\mathrm{d}E \quad (3)$$

where $N_{s\uparrow}$ and $N_{s\downarrow}$ are the Zeeman-split superconducting DOS and $f'(E)$ is the derivative of the Fermi function. The spin polarization of the tunnelling current can then be determined from the shape of an I–V curve:

$$P_T = \frac{I_\uparrow - I_\downarrow}{I_\uparrow + I_\downarrow} = \frac{N_\uparrow(E_F)\left|M_\uparrow(E_F)\right|^2 - N_\downarrow(E_F)\left|M_\downarrow(E_F)\right|^2}{N_\uparrow(E_F)\left|M_\uparrow(E_F)\right|^2 + N_\downarrow(E_F)\left|M_\downarrow(E_F)\right|^2}, \quad (4)$$

where $I_\uparrow(I_\downarrow)$ is the fraction of majority (minority) electrons in the tunnel current. This result was stated explicitly by Tedrow and Meservey in [22], and more recently by Worledge and Geballe when they discussed their tunnelling measurements of the spin polarization in

LSMO [23]. Different interpretations of the tunnelling spin polarization (4) stems from the work of Stearns [24] in which she assumed the same nearly parabolic bands for both majority and minority electrons. Only with this assumption, the tunnelling spin polarization will be equal to the DOS spin polarization:

$$P_{\mathrm{T}} = P_0 = \frac{N_{\uparrow}(E_{\mathrm{F}}) - N_{\downarrow}(E_{\mathrm{F}})}{N_{\uparrow}(E_{\mathrm{F}}) + N_{\downarrow}(E_{\mathrm{F}})}.$$

However, as can be shown in the simplest case of a spatial barrier, tunnelling matrix elements can be described in terms of Fermi velocities [20] and thus even for conventional ferromagnets, such as Ni, Fe or Co, the simplified result is not true, as the Fermi velocities are very different for spin-up and spin-down (s- and d-) electrons.

In summary, we would like to emphasize that we cannot talk about the spin polarization of a solely magnetic material incorporated into a tunnel junction. We should consider it together with the tunnel barrier; the same material may have a different P with different barriers, as well as with different counter-electrodes.

6. Point-contact Andreev reflection (PCAR) technique

The PCAR technique is based on Andreev reflection [25], which is a process taking place at the interface between a normal metal and a superconductor, which allows the propagation of a single electron with the energy below the superconducting gap from the normal metal to the superconductor, or rather a conversion of a quasi-particle current into a super-current. This process can also be described as *reflection* or *retro-reflection* of a hole (with the opposite spin), as the hole (approximately) retraces the trajectory of the incident electron. In a non-magnetic material, AR is always allowed, because the Fermi surfaces for majority and minority electrons are identical and every energy state has both spin-up and spin-down electrons. In a ferromagnet the two Fermi surfaces are no longer the same, due to the exchange splitting and AR being limited by the minority spin population[3]. In the idealized case of a perfect half-metal it is completely forbidden (at $T = 0$ K), as there are no states for a hole to get reflected to. This results in a *zero* conductance across the interface at the bias voltage below the gap. The classical theory of AR was developed by Blonder, Tinkham, and Klapwijk (BTK) and [26, 27], who assumed ballistic transport across the interface, which can be implemented when the two conductors are separated by a constriction (point contact). In the ballistic case the problem may be significantly simplified by assuming that: (a) the superconducting order parameter rises from zero to Δ_0 within a distance a from the interface[4] and thus can be modelled by a step function ($\Delta = \Delta_0$ inside the superconductor and 0 outside); (b) all the voltage drop also occurs within a distance a from the interface [29]. While these assumptions are somewhat arbitrary, and a rigorous approach should include self-consistent determination of the potential and order parameter variation across the interface, they, together with the assumption of a specular (δ-function) barrier at the interface, significantly simplify the calculations.

The PCAR technique makes use of a correlation between the degree of suppression of AR at a metal–superconductor interface and the (transport) spin polarization of the metal, P_1 or P_2. Namely, if one is able to measure the conductance of a point contact [30] or a nanocontact [31] (the simplest geometry to observe AR) at the interface with an unknown material, one can determine the spin polarization of this material from the overall shape of the

[3] More precisely, it is limited by the number of overlapping minority and majority conductivity channels.

[4] This assumption is justified for a three-dimensional (3D) contact, as it can be shown that the constriction makes the gap rise on a scale comparable to the size of the contact, a, which is typically much less than the coherence length, ξ; see [28]. In 1D–2D, the gap changes much more gradually.

conductance curve[5]. Quantitatively, the total current across the metal–superconductor interface can be decomposed into the fully spin-polarized current I_p and the unpolarized part of the current, I_u [30]. The unpolarized fraction of the current can be treated exactly as in the BTK paper [26]. The case for I_p was solved in [32], where the BTK approach was extended over the half-metallic conduction channels. Each half-metallic channel corresponds to a certain value of quasi-momentum in the direction parallel to the interface, k_{II}, allowed in one of the channels. In the unpolarized case the incoming electron with energy $E < \Delta$ propagates into the classically forbidden region as an evanescent wave [26] and thus is transformed into a Cooper pair within a distance on the order of a coherence length ξ. Somewhat similarly, in the fully polarized (half-metallic) case, while the AR current does not flow, the AR hole can exist as an evanescent wave, changing the transparency of the channel at $eV > \Delta$. Importantly, a simple renormalization of the normal current by setting the AR coefficient to zero at $eV > \Delta$, as was done in [30], leads to a different result. A complete set of formulae needed to analyse experimental curves obtained in the PCAR experiments is derived in [32].

7. Spin polarization and magnetoresitance of LSMO

The family of manganese perovskites, $La_{1-x}A_xMnO_3$ (A = Ca, Ba, or Sr), which is also known, because of its colossal magnetoresitance, as CMR oxides, has attracted intense interest in recent years due in part to their possible device applications and in part to their highly unusual structural, magnetic and electronic properties, which have presented theory with a formidable challenge. Their interdependent magnetic and electronic properties, including the spin polarization, are determined by the position of the Fermi level and the details of the p–d hybridization in the majority and minority bands. Therefore, the values of the spin polarization are extremely sensitive to the band structure of the compound. Half-metallicity has been predicted theoretically in many different materials (see, e.g., [7, 8, 33, 34]), yet the experimental confirmation of this effect (even at $T = 0$ K) is still quite controversial, especially for LSMO. Theoretical [35] and experimental values [36–39] of the spin polarization of this fascinating material obtained by different techniques varied widely from ∼35% to ∼100%. When the conclusion that LSMO is completely (100%) spin polarized was drawn, based on spin-resolved photoemission spectroscopy measurements [36], it attracted immediate attention. Indeed, this conclusion disagreed strongly with the band structure calculations [35], which predicted just 36% for the DOS spin polarization of the bulk $La_{0.7}Ca_{0.3}MnO_3$ ($La_{0.7}Sr_{0.3}MnO_3$), P_0, which presumably is the quantity measured in the photoemission experiments. Measurements of LSMO/insulator/LSMO tunnel junction TMR reported by two groups [37, 38] also indicate incomplete (54% and 81%, respectively) spin polarization in $La_{0.66}Sr_{0.34}MnO_3$. The measurements of spin polarization in LSMO using the Meservey–Tedrow technique produced the value of 72% [39]. Since for a true half-metal, measurements performed by any technique should result in 100% (within the experimental error) spin polarization, the experimental and theoretical situation was rather puzzling. In order to resolve this controversy, systematic measurements of the spin polarization of LSMO epitaxial films (as-grown as well as irradiated) and bulk single crystals were conducted using the PCAR technique [1]. While very high spin polarization values (∼90%) were recorded for some of the samples, a direct correlation was found between P and the residual resistivity of the samples, ρ. The observed correlation between P and ρ, as opposed to the anticorrelation expected for a true half-metal due to spin-flip scattering and other decoherence effects, strongly suggests that, while the current

[5] In the *ballistic* limit and for a *clean* interface ($Z = 0$), the spin polarization can be estimated directly from the normalized conductance at zero bias, $P = 1 - G(0)/2G_n$.

spin polarization in LSMO can be very high (which is consistent with the large reported TMR values), LSMO does have minority spin states at the Fermi level. These results account for the wide variation in the reported spin polarization values, and are in good agreement with the band structure calculations [35]. While such a material is *not* a conventional half-metal, as $N_{\downarrow}(E_F) \neq 0$, 96% of the current in bulk $La_{0.7}Sr_{0.3}MnO_3$ is transferred by the majority electrons, so it can be called *a transport half-metal* [1].

8. LSMO samples

Using the PCAR technique, both LSMO bulk crystals and thin films were studied [1]. The bulk crystals were grown by a floating-zone technique [40]. The films in that study were grown on (100)-oriented $NdGaO_3$, MgO, and $LaAlO_3$ substrates by pulsed laser deposition and off-axis sputtering [41]. The composition was determined by x-ray fluorescence with an accuracy of approximately 5%. The growth conditions (deposition rate and substrate temperature) were tuned in order to fabricate films of the same composition but with different defect concentrations, and thus different residual resistivity, which was in the range from $\rho \sim 40$ to $\rho \sim 2000$ $\mu\Omega$ cm. Additional samples were obtained by irradiating the low-resistivity films with 10 MeV Si ions, which resulted in higher residual resistivity. Thus a subset of samples was obtained with presumably the same microstructure but different residual resistivity due to a different point defect concentration. Note that the lowest-resistivity samples used in [1] have a Curie temperature of ∼350 K and a coercive force of ∼50 G, and a residual resistivity of ∼40 $\mu\Omega$ cm, which is very similar to the sample used in the photoemission measurements of [36].

9. PCAR spin polarization measurements

In the PCAR measurements a point contact was established between an LSMO sample and a superconducting (Sn) tip. The measurements were performed in liquid He^4 to improve the temperature stability and uniformity and to reduce any possible heating effects. The I–V and dI/dV curves were obtained using the standard lock-in detection technique in the temperature range 1.5–4.2 K. At least ten point-contact junctions with different contact resistances, R_n, were established and studied. The typical contact resistance was of the order of 30 Ω, and was generally well within the limits $100\ \Omega > R_n > 1\ \Omega$ [42]. The normalized conductance, $G(V)/G_n$, was then calculated using G_n obtained for voltages $V \gg \Delta/e$. Each normalized curve was then fitted with the model [32] to obtain the value of the spin polarization. The details of the measurements and the analysis can be found in [1, 30, 43].

10. Temperature dependence of the spin polarization

As a first test of the PCAR technique, the conductance $G(V)/G_n$ for a single contact was measured at different temperatures from approximately 1.5 K to the superconducting transition temperature of Sn, $T_c \sim 3.7$ K. A strong temperature dependence of the normalized conductance was observed (figure 2): the curves were highly nonlinear as a function of voltage at the lowest temperatures[6] and nearly featureless close to T_c. Qualitatively, it is due to the fact that at higher temperatures the quasi-particle density in the superconductor increases, making possible the transmission of the quasi-particle current, and thus reducing the AR contribution.

[6] The change in conductance below the gap is due to the temperature dependence of both the quasi-particle density and the probability of Andreev reflection.

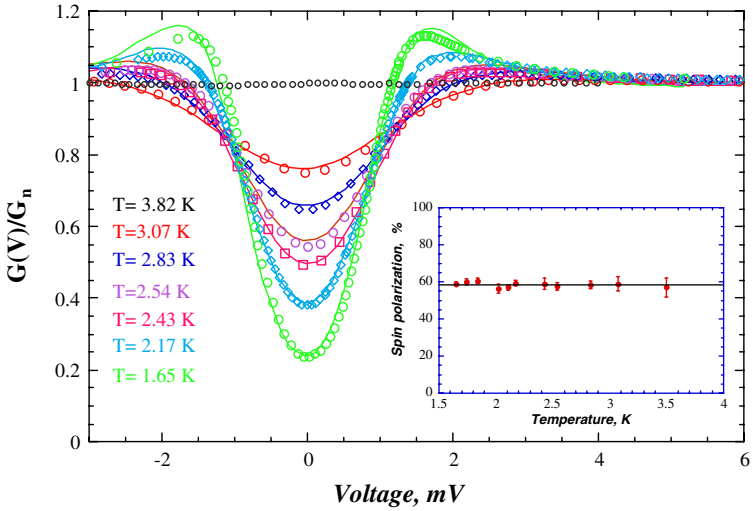

Figure 2. Experimental data and the fits (according to [32]) at different temperatures for $La_{0.7}Sr_{0.3}MnO_3$ films. Inset: temperature dependence of the spin polarization values for the same sample at 1.6 K $< T <$ 4.2 K.

For all $G(V)/G_n$, the conductance at $V = 0$ was *smaller* than at large voltages, indicating (for $Z \ll 1$) that the sample is fairly highly spin polarized[7]. Normalized $G(V)/G_n$ curves for every temperature were fitted using only two adjustable parameters: the spin polarization, P, and the barrier strength, Z (see figure 2). The superconducting gap, $\Delta(T)$, has never been used as a free parameter; rather it was determined separately from the known BCS (Bardeen–Cooper–Schrieffer) temperature dependence. We see that: (1) all of the experimental data can be fairly well described by this fitting procedure (based on [32]); and (2) despite the drastic change in $G(V)/G_n$ with temperature, the values of P for the same sample were practically independent of T (see the inset in figure 2). This is, of course, expected in this temperature range, as the Curie temperature of LSMO is much higher than the measurement temperature. Some of the lowest-resistivity samples were selected for these measurements to ensure the ballistic transport regime.

11. Overview of the spin polarization results in LSMO

The fact that the spin polarization values were found to be temperature independent at low temperatures was very encouraging, as it confirmed the consistency of the PCAR technique. Then the systematic measurements of the spin polarization in a number of $La_{0.7}Sr_{0.3}MnO_3$ thin films and bulk single crystals, whose residual resistivity ranged from 40 to 2000 $\mu\Omega$ cm, were carried out. Initially the results were rather disappointing, as very different values of the spin polarization were measured for different samples (ranging from ∼60% to ∼90%). Yet, when plotted as a function of a residual resistivity, the monotonic dependence was observed. Somewhat surprisingly, however, the transport spin polarization was found to be higher for the 'dirtier' samples, i.e. the samples with larger residual resistivity (see figure 3). Intuitively, one would expect the trend to be just the opposite; a higher spin polarization for the 'better' samples with a longer mean free path. Indeed, if the material was a true half-metal, better

[7] For $Z = 0$ the normalized conductance at $V = 0$ is equal to $2(1 - P)$.

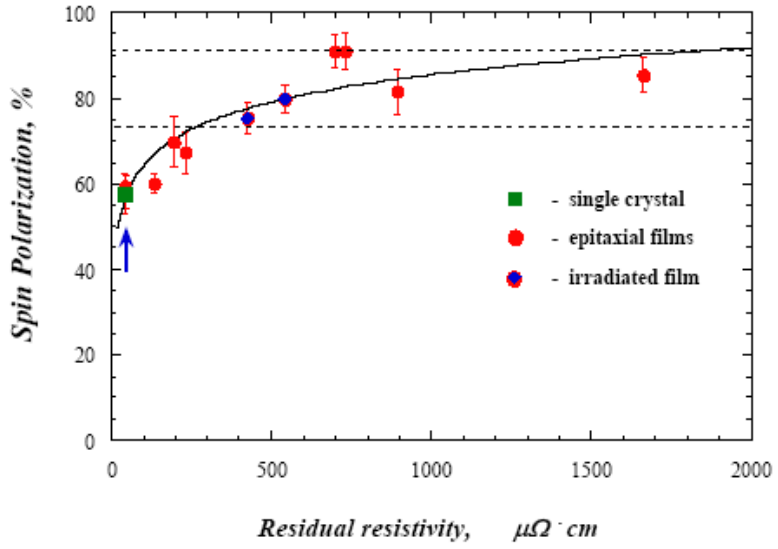

Figure 3. Spin polarization as a function of residual resistivity of $La_{0.7}Sr_{0.3}MnO_3$ films and single crystals at $T = 1.6$ K: ●, epitaxial films; ■, single crystal; ●, irradiated films, the lowest-resistivity film before (after) irradiation with Si ions. Dashed lines correspond to $P_1 = 74\%$ and $P_2 = 92\%$ (see text). Solid lines are guides to the eye.

samples would have had less spin-flip scattering and thus would exhibit spin polarization close to 100%, as was the case, for instance, for CrO_2 [44]. The observed results can be understood, however, if we take into account the dependence of P on the transport regime which is determined by the ratio of the electronic mean free path to the contact size, as we discussed before. Overall, the possible values of P measured for all the samples should be confined between P_1 (pure ballistic limit) and P_2 (pure diffusive limit). Using the values of the densities of states ($N_\uparrow(E_F) = 0.58$ states/eV Mn, $N_\downarrow(E_F) = 0.27$ states/eV Mn) and Fermi velocities ($V_{F\uparrow} = 7.4 \times 10^5$ m s^{-1}, $V_{F\downarrow} = 2.2 \times 10^5$m s^{-1}) from [35], $P_1 = 74\%$, and $P_2 = 92\%$ were obtained, in fairly good agreement with the experimental data[8]. The value of P_2 which also corresponds to the spin polarization of the (bulk) current in LSMO implies that less than 5% of the current is carried in the spin-minority channel, so it can be assumed for an estimate that the conductance in LSMO is due entirely to the spin-majority channel. Using Ziman's expression for conductivity, $\sigma = \frac{1}{3}e^2N_\uparrow(E_F)V_{F\uparrow}^2\tau$, and $L = V_F\tau$, we obtain, for the three values of resistivity $\rho \sim 40$, ~400 and ~2000 $\mu\Omega$ cm, and, for the mean free paths, $L \sim 65$ nm, $L \sim 6.5$ nm, and $L \sim 0.65$ nm, respectively[9]. The contact size can be estimated from the normal resistance of the contact, R_n. Using a general expression [45],

$$R_n \approx \frac{4}{3\pi}\frac{\rho L}{a^2} + \frac{\rho}{2a}, \tag{5}$$

[8] The theory of [26], as well as its modified version [32], are based on the assumption of either ballistic transport, ($L \gg d$), or diffusive transport, ($L \ll d$). The theory for an arbitrary transport regime, $L \sim d$, has yet to be developed. However, the fact that one can apply the ballistic theory in the diffusive regime with no significant errors (2–3%) indicates that it is likely to be successful for the intermediate case as well.

[9] Note that Ziman's expression is only valid until k remains a good quantum number (and the Bloch–Boltzmann approach can still be applied). In the limit of very high defect concentrations (short mean free paths) when the conductivity is approaching the Mott localization limit, it can only be used as an approximation (see the discussion in section 12).

where ρ is the residual resistivity and a is the contact size. If we solve this equation for the contact size, using the typical experimental values of ρ and R_n for the lowest-resistivity samples with $\rho \sim 40$ $\mu\Omega$ cm, we obtain $a \sim 5$–7.5 nm. Therefore, these samples are in the ballistic regime and the measured values of the transport spin polarization should correspond to P_1. The resistivity range $\rho \sim 400$ $\mu\Omega$ cm corresponds to the intermediate regime ($L \sim a$), whereas the highest-resistivity samples, $\rho \sim 2000$ $\mu\Omega$ cm, are in the diffusive regime ($L \ll a$). These estimates are consistent with the results describe above.

12. Types of defects and residual resistivity of LSMO

In perovskites the variation in the oxygen content, the presence of grain boundaries, or other extraneous defects might often dominate the changes in residual resistivity. Therefore, it was important to make sure that, for the samples used in [1], the types of defects affected residual resistivity through the changes in the mean free path. Firstly, the chemical composition of the samples was determined by x-ray fluorescence with an accuracy of approximately 5%. Secondly, the extended x-ray absorption fine structure (EXAFS) measurements were performed to probe the local structure of LSMO directly. Specifically, the measurements of the Mn K-absorption edge, which give a quantitative description of the real-space local environment around the Mn atoms, were performed in order to reconstruct the MnO_6 octahedra in LSMO [46]. These measurements on films and bulk single crystals are described in detail in [1], where it was found that, in all of these samples, MnO6 octahedra experienced little or no distortion. On the other hand, these measurements indicated that the length of the Mn–La/Sr bond changed from site to site, likely due to the La/Sr site defects which are known to occur in LSMO, as was shown in the neutron diffraction experiments [47]. These variations are seen in the Mn–La/Sr correlation, where the amplitude of the corresponding Fourier peak systematically decreased with increasing residual resistivity in the range from 40 to 800 $\mu\Omega$ cm. The changes in the amplitude of this peak (the amplitude of the nearest-neighbour oxygen peak remained unchanged) are consistent with an increase in A-site cation defects with increasing residual resistivity. Such defects are likely due to octahedral rotation or tilting, without necessarily introducing any local distortion. Defect concentrations estimated from the EXAFS experiments correlate with the residual resistivity, demonstrating that it is these defects which are mostly responsible for electron scattering. Thus the observed monotonic dependence of the spin polarization on the residual resistivity is due to the changes in the carrier mean free path and is not related to the microstructure or possibly the slight variation in chemical composition in different samples.

Finally, one of the low-resistivity films was irradiated with a gradually increasing dose of 10 MeV Si ions. Then measurements of P were performed as a function of resistivity in a set of samples which were *nominally identical*, except for the number of defects. Qualitatively, the effect was the same: the spin polarization increased as a result of irradiation. The spin polarization values for the irradiated sample, however, seem to deviate from the curve for as-grown films and crystals (see figure 3). This is not surprising, as the conductivity is mostly (∼95%) determined by the spin-majority band, while the spin polarization is effectively controlled by the minority band, and different defects (irradiation and growth defects) do not, generally, affect the two bands in the same way. Due to the large difference between the two bands, the same defects are likely to influence the transport in the minority band more strongly, as it is can potentially approach the so-called minimal metallic conductivity limit, $k_F L \sim 1$. In this case, the defects will dramatically modify the minority carrier properties, without significantly affecting the majority carriers. Eventually, while the majority carriers retain a reasonable mean free path to maintain the current at low temperatures, the minority

carrier may be localized by the disorder, in which case the transport spin polarization will approach 100%.

How can one interpret these results? The physical picture that we have in mind is the following: when we have relatively low-defect, low-resistivity samples with a mean free path L about an order of magnitude higher than the minimum contact size a, we can easily establish a ballistic contact. As the number of defects in a sample goes up (or, in the case of irradiated samples, additional radiation defects are intentionally introduced), the resistivity goes up and the mean free path is reduced; as L approaches the contact size, we can no longer have a purely ballistic contact and we are in the intermediate regime. As the number of defects reaches the maximum level at which it is still possible to perform the measurements (roughly on the order of mΩ cm), we are in a purely diffusive regime. One can argue that it should still be possible to establish a diffusive contact even in the case of low-resistivity samples (long mean free path) by simply increasing the size of the contact. However, in the case of a point contact, it is not so easy to do it since, instead of a single large contact, a number of smaller contacts (in parallel) will typically be established [48]. Our analysis would have been in serious trouble had the extracted values of spin polarization depended strongly on whether we use a diffusive or ballistic model, simply because it is not always easy to unambiguously deduce if you are in the ballistic or the diffusive regime, particularly close to a crossover point. Fortunately, as it turned out, the extracted values of the spin polarization are practically independent of the model, as was shown by Woods *et al* [49]. In fact, the errors introduced by interchangeably using these two models are limited by ∼3%, which is approximately two times smaller than the errors introduced from incorrect renormalization in the half-metallic case discussed in section 6.

13. Transport spin filtering

Importantly, we note that the values of P obtained by the PCAR technique are only single valued if a particular *experimental* transport (e.g. ballistic) regime is maintained. Consequently, one can change the degree of spin polarization (of the current) by simply changing *the contact geometry*, as the value of spin polarization changes in the case of ballistic-to-diffusive contact transition, as seen for example for LSMO (figure 4). In figure 4(a), a constriction with the electron mean free path L larger than the size of the constriction a, is shown. If we reduce the mean free path L, or equivalently increase the size of the constriction a (as shown in figure 4(b)), then we are in the diffusive transport regime and $P = P_2$. Depending on the ratio of the Fermi velocities and the densities of states for majority and minority carriers, we may see a significant change in spin polarization (from 58% to 88%, as was observed for LSMO, for instance). This effect can be called transport spin filtering. A good thermodynamics analogy would be a transition between a ballistic (Knudsen) flow through a pinhole, in which equilibrium between the two volumes is determined by a particle flux from both sides of $\sim n\langle v\rangle$ and a diffusive (hydrodynamic) flow in which equilibrium is determined by a pressure $\sim T \sim \langle v^2\rangle$, thus having a quadratic dependence on velocity. Therefore, one can also change the value of the spin polarization of the current by simply changing the size of the constriction for a given mean free path of the electrons (see figure 4). A similar effect is true, of course, in the case of the Meservey–Tedrow technique, which is sensitive not only to the band structure of the ferromagnet but to the spin selectivity of the tunnel barrier. So, one can suppress or enhance the spin filtering effects of the tunnel junction by adjusting the relative transparency of the barrier for the majority and minority electrons [50], which has been demonstrated in the case of Al_2O_3 and MgO barriers for Co TMR junctions [10].

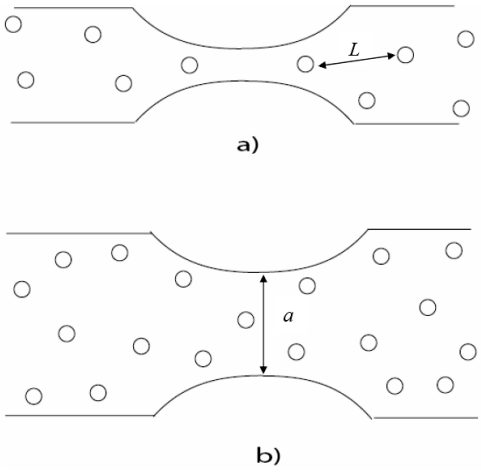

Figure 4. Transport spin filtering: the value of spin polarization depends on the transport regime: in the ballistic regime ($L > a$), $P = P_1$; in the diffusive regime ($L < a$), $P = P_2$, the same is true for no-constriction, bulk Bloch–Boltzmann spin transport. The spin polarization can be controlled by changing the geometry (size) of the contact a, without changing the mean free path L: (a) $a < L$ (ballistic case); (b) $a > L$ (diffusive case). In the case of LSMO, $P_1 \sim 60\%$, while $P_2 \sim 90\%$.

14. Comparison with the other experiments and conclusions

More recently, the PCAR technique was used by another group to measure LSMO single crystals [51], finding $P = 78\%$. There results are in qualitative agreement with [1], as well as the tunnelling measurements of [37–39] and the band structure calculations [35], indicating that LSMO in not a half-metal. How can this be reconciled with the 100% polarization photoemission data [36]? First, we note that the lowest-resistivity samples described above are very close to the sample from [36]. They have practically identical resistivity, Curie temperatures and coercive forces. On the other hand, band structure calculations, which agree surprisingly well with the transport measurements, predict for the photoemission-probed spin polarization, P_0, only about 35%. Since roughly just a 10 Å surface layer is accessible to photoemission [36], one might assume that only the surface of the sample, which had undergone a complex cleaning procedure [36], was half-metallic. Since the surface atom has a smaller coordination number, Z, to a bulk atom, it is quite natural to assume that one of the main surface effects on the electronic structure is the band narrowing [1], by ∼20% for the cubic perovskite lattice[10]. The overall bandwidth, which is roughly proportional to Zt (where t is the effective hopping integral), is reduced at the surface by the same amount. While surface relaxation effects may change the hopping integral t, thus partially offsetting the reduction of the coordination number, the net effect on the total bandwidths is usually negative. As the minority band in LSMO is quite narrow and its edge is very close (∼0.2 eV) to the Fermi energy, band narrowing can easily make the system half-metallic. To estimate whether surface-induced band narrowing of the order of 20% might be responsible for the results of [6], a similar situation was considered [1]. Specifically, the effect of the uniform expansion on the band structure of LSMO was calculated in the virtual crystal approximation. In this case, the bands narrow due to the reduction in t, not Z, which is obviously unchanged. It was found

[10] In *layered* perovskites, where the bandwith is due predominantly due to in-plane hopping, one does not expect surface band narrowing, and indeed *ab initio* calculations show a very small surface effect in layered $LaSr_2Mn_2O_7$ [52].

that just a 3% linear expansion, which corresponds to a ∼10% reduction[11] in t and thus to a ∼10% reduction in the overall bandwidth, is sufficient to make the system half-metallic [1]. Therefore, it is plausible that the surface layer of LSMO is, indeed, half-metallic[12].

How does the transport half-metallicity stack up against some of the other recent experimental results? A very large TMR on the order of 1000–2000% was recently obtained for LSMO/STO/LSMO tunnel junctions (STO is $SrTiO_3$) [55], from which the authors inferred approximately 89–95% transport spin polarization for the LSMO/STO electrode. This result agrees well with the results of [1] ($P_2 = 88$–92%). At the same time, it does not indicate that LSMO is a conventional half-metal. Another very interesting effect was observed in trilayer LSMO/Ba_2LaNbO_6/LSMO [56], where temperature and bias inversion of the sign of TMR was observed for the same tunnel junction. The authors of [56] explain this effect by assuming that they have transport through nanoscale metallic channels, in parallel with conventional tunnelling through an oxide layer. This picture relies heavily on the fact that there are minority spin states in LSMO, serving as indirect proof of their existence.

In summary, some of the recent transport studies confirm that LSMO can have a very high degree of current spin polarization (on the order of 90%), consistent with the earlier observations of [1]. At the same time, the presence of minority electrons at the Fermi level in LSMO has been deduced from inverse TMR with pinhole nanocontacts [56]. These and other recent results confirm our earlier picture of $La_{0.7}Sr_{0.3}MnO_3$ as a transport half-metal, with transport spin polarization approaching 100% in the high-resistivity (or tunnel junction) limit. The origin of this high spin polarization (spin-majority electrons carry ∼96% of the current) is mostly related to the large difference in the mobility of the spin-up and spin-down electrons, rather than their DOS. Our conclusions are based not so much on the measured spin-polarization values, but on the observation of an unambiguous correlation between the residual resistivity of LSMO and its spin polarization, which is *opposite* to the one expected for a true half-metal.

Acknowledgments

The author is grateful to I I Mazin and A Petukhov for useful suggestions. The work is supported by the US National Science Foundation (NSF) ECCS-0239058 CAREER and Office of Naval Research (ONR) grant N00014-06-0439.

References

[1] Nadgorny B, Mazin I I, Osofsky M, Soulen R J Jr, Broussard P, Stroud R M, Singh D J, Harris V G, Arsenov A and Mukovskii Ya 2001 *Phys. Rev.* B **63** 184433
[2] de Groot R A, Mueller F M, van Engen P G and Buschow K H J 1983 *Phys. Rev. Lett.* **50** 2024
[3] Eschrig H and Pickett W E 2001 *Solid State Commun.* **118** 123
[4] Dowben P A and Skomski R 2004 *J. Appl. Phys.* **95** 7453
Skomski R and Dowben P A 2002 *Europhys. Lett.* **58** 544
[5] Irkin V Yu and Katsnelson M I 2006 *Phys. Rev.* B **73** 104426
[6] Orgassa D, Fujiwara H, Schulthess T C and Butler W H 1999 *Phys. Rev.* B **60** 13237
[7] Pickett W E and Moodera J S 2001 *Phys. Today* **54** 39
[8] Zutic I, Fabian J and Das Sarma S 2004 *Rev. Mod. Phys.* **76** 323
[9] Juliere M 1975 *Phys. Lett.* A **54** 225–6

[11] According to the Harrison scaling rule, the pd hopping scales with the bond length, a, as $a^{-3.5}$ [53].
[12] Additionally, the photoemission measurements can be affected by spin filtering, whereby a faster scattering rate for minority spin electrons compared to the majority spin electrons leads to an excessive apparent spin polarization (see [54]). This explanation is also consistent with the lack of dispersion, $E(k)$, observed in [36].

[10] Parkin S S P, Kaiser C, Panchula A, Rice P M, Hughes B, Samant M and Yang S-H 2004 *Nat. Mater.* **3** 862–7
[11] Dyakonov M I and Perel V I 1971 *Phys. Lett.* A **35** 459
[12] Jonker B T, Hanbicki A T, Pierce D T and Stiles M D 2004 *J. Magn. Magn. Mater.* **277** 24
[13] Mazin I I 1999 *Phys. Rev. Lett.* **83** 1427
[14] van de Veerdonk R J M, Moodera J S and de Jonge W J M 1997 *Conf. Digest of the 15th Int. Colloquium on Magnetic Films and Surfaces (Queensland, Aug. 1997)* (unpublished)
[15] Monsma D J and Parkin S S P 2000 *Appl. Phys. Lett.* **77** 720
[16] Nadgorny B *et al* 2000 *Phys. Rev.* B **61** R3788
[17] Gudenko S V and Krylov I P 1984 *Zh. Eksp. Teor. Fiz.* **86** 2304
Gudenko S V and Krylov I P 1984 *Sov. Phys.—JETP* **86** 2304 (Engl. Transl.)
[18] Parker J S, Watts S M, Ivanov P G and Xiong P 2002 *Phys. Rev. Lett.* **88** 196601
[19] Sharvin Yu V 1965 *Sov. Phys.—JETP* **21** 655
[20] Mazin I I, Golubov A A and Zaikin A D 1995 *Phys. Rev. Lett.* **75** 2574
[21] De Teresa J M, Barthélémy A, Fert A, Contour J P, Montaigne F and Seneor P 1999 *Science* **286** 507
[22] Meservey R and Tedrow P M 1994 *Phys. Rep.* **238** 173
[23] Worlege D C and Geballe T H 2000 *Phys. Rev.* B **62** 447
[24] Stearns M B 1977 *J. Magn. Magn. Mater.* **5** 167
[25] Andreev A F 1964 *Sov. Phys.—JETP* **19** 1228
[26] Blonder G E, Tinkham M and Klapwijk T M 1982 *Phys. Rev.* B **25** 4515
[27] A similar approach was used by Demers J and Griffin A 1970 *Can. J. Phys.* **285** 49
[28] Likharev K K and Yakobson L A 1976 *Sov. Phys.—JEPT* **41** 570
[29] Kulik I O, Omel'yanchuk A N and Shekhter R I 1977 *Sov. J. Low Temp. Phys.* **3** 740
[30] Soulen R J Jr, Byers J M, Osofsky M S, Nadgorny B, Ambrose T, Cheng S F, Broussard P R, Tanaka C T, Nowak J, Moodera J S, Barry A and Coey J M D 1998 *Science* **282** 85–8
[31] Upadhyay S K, Palanisami A, Louie R N and Buhrman R A 1998 *Phys. Rev. Lett.* **81** 3247
[32] Mazin I I, Golubov A A and Nadgorny B 2001 *J. Appl. Phys.* **89** 7578
[33] de Groot R A and Buschow K H J 1986 *J. Magn. Magn. Mater.* **54** 1377
[34] Schwarz K J 1986 *J. Phys. F: Met. Phys.* **16** L211–5
[35] Pickett W E and Singh D J 1996 *Phys. Rev.* B **53** 1146
[36] Park J-H *et al* 1998 *Nature* **392** 794
[37] Lu Y *et al* 1996 *Phys. Rev.* B **54** R8357
[38] Sun J Z *et al* 1997 *Appl. Phys. Lett.* **70** 1769–71
[39] Worlege D C and Geballe T H 2000 *Appl. Phys. Lett.* **76** 900
[40] Shulyatev P *et al* 1999 *J. Cryst. Growth* **199** 511
[41] Broussard P R, Qadri S Q, Browning V M and Cestone V C 1997 *Appl. Surf. Sci.* **115** 80
[42] Blonder G E and Tinkham M 1983 *Phys. Rev.* B **27** 112
[43] Panguluri R, Tsoi G, Nadgorny B, Chun S H and Samarth N 2003 *Phys. Rev.* B **68** R 201307
[44] Anguelouch A, Gupta A, Xiao Gang, Abraham D W, Ji Y, Ingvarsson S and Chien C L 2001 *Phys. Rev.* B **64** 180408
[45] Wexler G 1966 *Proc. Phys. Soc. London* **89** 927
The exact solution for an arbitary case can be found in Nikolić B and Allen P B 1999 *Phys. Rev.* B **60** 3963
[46] Rehr J J, Albers R C and Zabinsky S I 1992 *Phys. Rev. Lett.* **69** 3397
[47] Mitchell J F, Argyriou D M, Potter C D, Hinks D G, Jorgensen J D and Bader S D 1996 *Phys. Rev.* B **54** 6172
[48] Bugoslavsky Y, Miyoshi Y, Perkins G K, Caplin A D, Cohen L F, Pogrebnyakov A V and Xi X X 2005 *Phys. Rev.* B **72** 224506
[49] Woods G T, Soulen R J, Mazin I, Nadgorny B, Osofsky M S, Sanders J, Srikanth H, Egelhoff W F and Datla R 2004 *Phys. Rev.* B **70** 054416
[50] Butler W H, Zhang X-G, Schulthess T C and Macharen J M 2001 *Phys. Rev.* B **63** 054416
[51] Ji Y, Chien C L, Tomioka Y and Tokura Y 2002 *Phys. Rev.* B **66** 012410
[52] de Boer P K and de Groot R A 1999 *Phys. Rev.* B **60** 10758
[53] Harrison W A 1980 *Electronic Structure and the Properties of Solids* (SanFrancisco, CA: W H Freeman)
[54] Penn D R, Apell P S and Girvin S M 1985 *Phys. Rev. Lett.* **55** 518
Pappas D P *et al* 1991 *Phys. Rev. Lett.* **66** 504
[55] Bowen M, Bibes M, Barthélémy A, Contour J-P, Anane A, Lemaître Y and Fert A 2003 *Appl. Phys. Lett.* **82** 233
[56] Mukhopadhyay S and Das I 2006 *Phys. Rev. Lett.* **96** 026601